Extreme Mechanics Letters 45 (2021) 101284

Contents lists available at ScienceDirect

Extreme Mechanics Letters

journal homepage: www.elsevier.com/locate/eml

Advances in experimental mechanics at atomic scale

Sixue Zheng, Scott X. Mao *

Department of Mechanical Engineering and Materials Science, University of Pittsburgh, Pittsburgh, Pennsylvania 15261, USA

ARTICLE INFO

Article history:
Received 21 December 2020
Received in revised form 8 February 2021
Accepted 12 March 2021
Available online 18 March 2021

Keywords:
In situ transmission electron microscopy
Atomic scale
Small-sized materials
Mechanical behaviors

ABSTRACT

With the ongoing trend of miniaturizing electronic devices, the dimensions of metallic materials used in these devices decrease continuously from sub-microns to a few nanometers. Small-sized materials usually exhibit superior mechanical properties and dramatically different mechanical behaviors from their bulk counterparts. Deep insights into the atomistic mechanical behaviors in small-scale metals are of vital importance for designing new nanostructured materials to guarantee the reliability and stability of future nanodevices. This review firstly presents state-of-the-art experimental techniques and sample preparation methods for atomic-scale *in situ* deformation dynamics on small-sized metals. Then, recent advances in atomic-scale experimental mechanics are summarized, including size-dependent defect nucleation, twinning-related mechanism, phase transformation, diffusional deformation and pseudoelasticity. Finally, current limitations and future directions for research in the field of atomistic experimental mechanics are discussed.

Published by Elsevier Ltd.

1. Introduction

Small-sized metal materials have been widely used in a variety of inherently small structures, such as micro/nanoelectromechanical systems (M/NEMS) [1,2], micro/nanosensors [3], electronic skin [4,5] and flexible electronics [6]. In these microelectronic assemblies, the metal materials with characteristic size ranging from microns to nanometers, are employed as electrodes and interconnect due to their excellent electrical conductivity and strength [5,7,8]. Mechanical degradation, however, occurred frequently in these small-scale materials under various forms of mechanical loading and then deteriorated electrical performances, which makes their reliability the biggest challenge in the practical application of electronic devices. Thus, profound insights into the mechanical behaviors of micro- and nanosized metal materials are of importance not only for designing structurally stable materials to guarantee the reliability of micro- and nanoscale devices but also for a fundamental understanding of the mechanisms governing plasticity at small scale [9].

Due to the extremely small dimensions, investigating the mechanical behaviors of nanostructured materials can be technically demanding. So far, the atomic-scale understanding of the mechanical behaviors in nanostructured materials have been relying heavily on Molecular dynamics (MD) simulations. Limited by computational resources, MD simulations are normally conducted at strain rates (usually 10^7–10^9/s), which is at least 10 orders of magnitude higher than the quasistatic experimental strain rates (typically 10^{-3}–10^{-4}/s) [10,11]. Furthermore, MD simulations also suffered from the accuracy of empirical or semi-empirical interatomic potentials [12–14] and geometry of sample [15]. Because of these mismatches, it naturally raises questions whether or not the simulation results can be directly extrapolated to those under laboratory conditions. Powerful experimental studies are thus in urgent need to validate the research findings from computational investigations. Recently, advanced *in situ* mechanical testing methods with high-resolution transmission electron microscopy (HRTEM) were developed to visualize the dynamic mechanical deformation at nano or even atomic scale [16–19]. The sample dimensions studied by *in situ* TEM experiments are at the same order of those used in MD simulations, which allows to bridge the gaps between experiments and simulations. Particularly, TEM-based *in situ* nanomechanical experiments provide a unique opportunity to uncover new atomic-scale deformation mechanisms explicitly.

In this article, we firstly overview recent advances in *in situ* mechanical testing techniques by TEM. Subsequently, we systematically summarize recent progresses in the atomic-scale investigations on mechanical behaviors in small-sized metals, including length scale-dependent dislocation nucleation, twinning-related mechanism, phase transformation, diffusion-mediated deformation and pseudoelasticity. Finally, the prospect of future research about atomistic experimental mechanics will be discussed.

2. TEM-based *in situ* nanomechanical testing method

Because of the increasing technological prominence of nanostructured metal materials [20], the particularly small specimen

* Corresponding author.
E-mail address: sxm2@pitt.edu (S.X. Mao).

https://doi.org/10.1016/j.eml.2021.101284
2352-4316/Published by Elsevier Ltd.

size, the difficulty in ultra-low force load cell and lack of reliable clamping method led to an urgent demand for new-developed experimental methods to investigate their mechanical properties at small scale. Benefited from a number of recent technical developments, some *in situ* testing methods has been proposed and incorporated into various characterization platforms, including atomic force microscopy (AFM) [21,22], scanning electron microscopy (SEM) [23–26], TEM [27–29] and X-ray diffraction [30] etc. Among these advanced experimental methods, TEM-based *in situ* nanomechanical testing methods so far open new horizons toward characterizing and analyzing dynamical mechanical behaviors at atomic scale directly. Here, we overview relatively common sample preparation and mechanical testing techniques.

Small-volume specimens can either be fabricated from their bulk components (top-down method) or grown to a size (bottom-up method) that can be handled by holders and micromanipulators [17]. The classical top-down specimen in the micron or submicron diameter regime is fabricated by focused ion beam (FIB) milling. However, FIB cutting may introduce significant surface contamination and a large number of defects near surface [31,32] and modify the original microstructure [33], probably influencing intrinsic mechanical response. Bottom-up methods, such as physical vapor deposition (PVD) [26,34] and electrodeposition [17], were designed to prepare specimens from micrometer to nanometer scale (e.g., metallic nanowhiskers and nanowires). However, systematic defects and impurities may be induced during crystal growth [35]. Until very recently, an *in situ* thermal welding technique was proposed to fabricate high-quality metallic nanowires in TEM directly (see Fig. 1a) [36–40]. Specifically, numerous metal nano-tips were firstly generated at the clean fracture surface of bulk metallic substrates using a wire cutter and then loaded onto the static side and the probe side of the TEM holder (see Fig. 1b). The nano tips with selected zone axis approached each other by controlling the piezo-manipulator (see Fig. 1c) and then were welded together by applying a constant voltage (see Fig. 1d). These procedures generate bridge-shaped single crystals with clean surfaces, different dimensions and controllable orientations. Compared with the techniques mentioned above, such sample preparation method is generally applicable to a variety of material systems and ideal for studying atomistic mechanical behaviors of nanomaterials.

The key hurdle in conducting *in situ* TEM testing is the miniaturization of experimental setups, due to the fact that the space between the pole pieces in the TEM chamber are rather small ($\sim$3 mm) [19,35]. In order to meet this extreme operating condition, some effective *in situ* straining methods have been proposed by incorporating nanoindentation, MEMS-based testing device, AFM and scanning tunneling microscope (STM) probe into a TEM platform. Nanoindenter-based TEM holders are able to measure the force (in the order of μN) and displacement of a flat punch tip forced into the cylindrical nanopillars (see Fig. 1e) [18,42,43]. The contact of the tip with the pillar, however, generates strain gradients and thus disrupt imaging conditions during the deformation. MEMS-based testing platforms were developed to perform quantitative *in situ* TEM tensile tests, in which load is measured with 10 nN resolution and displacement with subnanometer resolution (see Fig. 1f) [19]. Most of these MEMS platforms, however, highly relied on quite complicated setups making their implementations and operations both challenging and expensive [24]. Besides, a AFM-TEM sample holder was developed for quantitative measurement of nanowire strength (see Fig. 1g) [44]. Clamping of the sample was carried out by pushing the coated nanowire on a STM probe against the AFM tip surface until strong bonding was formed. The applied force during testing can be calculated by the recorded deflection of the AFM cantilever with known spring constant. This testing method, however, failed to capture HRTEM images of nanocrystals to reveal atomic-scale deformation mechanisms due to unsatisfactory sample quality. In addition, *in situ* TEM straining methods using nanoindentation, AFM and MEMS devices were usually carried out on samples in the micron or submicron diameter regime [45]. Most importantly, these methods were hard to conduct high-quality atomic imaging due to the difficulties in varying sample orientation.

To solve the aforementioned difficulties in performing in situ TEM tests, Han et al. [46] specially designed a thermally actuated TEM tensile device (see Figure 1h), which is capable of investigating the grain boundary (GB)-mediated plasticity in nanocrystalline (NC) metals [27,29,47] and the mechanical behaviors of metallic nanowires [48,49]. The tensile device, loaded onto a TEM heating stage, consisted of two bimetallic strips, which were fixed, in opposing positions, on a TEM Cu-ring grid. Due to the difference in thermal expansion coefficients of different materials in bimetallic strips, the strips were bent in opposite directions to provide the tensile pulling force for the samples under heating conditions. Thus, the conventional TEM heating stage can operate as a double tilt, displacement controlled, deformation stage. Using the above method, the sample can be oriented in a desirable low-index crystallographic orientation for obtaining high-quality HRTEM imaging. The strain and strain rate applied to the sample can be controlled precisely using a temperature controller. In addition to the thermally actuated tensile device, the STM probe-based technique opened new avenues to investigate the mechanical behaviors of nanostructured materials systematically [35]. Pristine single nanocrystals with different size were attached to a metal rod, which is used as one end of the TEM stage. The STM probe, the other end of the TEM stage, can be connected to the sample inside a TEM using amorphous carbon deposition [15,22,50] and *in situ* thermal welding technique [36,38,51]. The applied strain during *in situ* testing can be calculated based on the difference in gauge length, which is selected according to the sample geometry [36]. The applied stress can be obtained by Young's modulus of metal materials and atomic-scale lattice strain measurements [15,22]. Besides, probe-based technique also allows to conduct high-temperature nanomechanical testing by controlling the Joule heating, which is generated by applying constant voltage on the two ends of the metallic nanocrystal. Consequently, compared with other testing methods, this testing technique has a capability of providing more useful information about mechanical deformation and obtaining high-quality TEM imaging.

3. Length scale-dependent dislocation nucleation

With the ongoing trend of miniaturizing materials in M/NEMS, the geometric and microstructural dimensions of the metal materials are normally in the range of microns to nanometers, which is of the same order as dislocation line length [52]. The constraints of the characteristic dimensions on dislocation activities and the pronounced surface effect caused by high surface-to-volume ratio in nanostructured metals result in the mechanical behaviors of nanostructured metals quite different from their bulk counterparts. For instance, superior strength is often achieved in small-scale metal materials, which is associated with a fundamental change in deformation process. *In situ* TEM nanomechanical testing provides a unique opportunity to observe the atomic-scale and time-resolved dynamics of defect nucleation, revealing new deformation mechanisms in small-sized samples. To date, dislocation nucleation process is found to be associated with the characteristic length scale of metal materials.

In bulk metals, dislocations are usually generated by Frank–Read source [53], grain boundary (GB) [54,55], the intersection

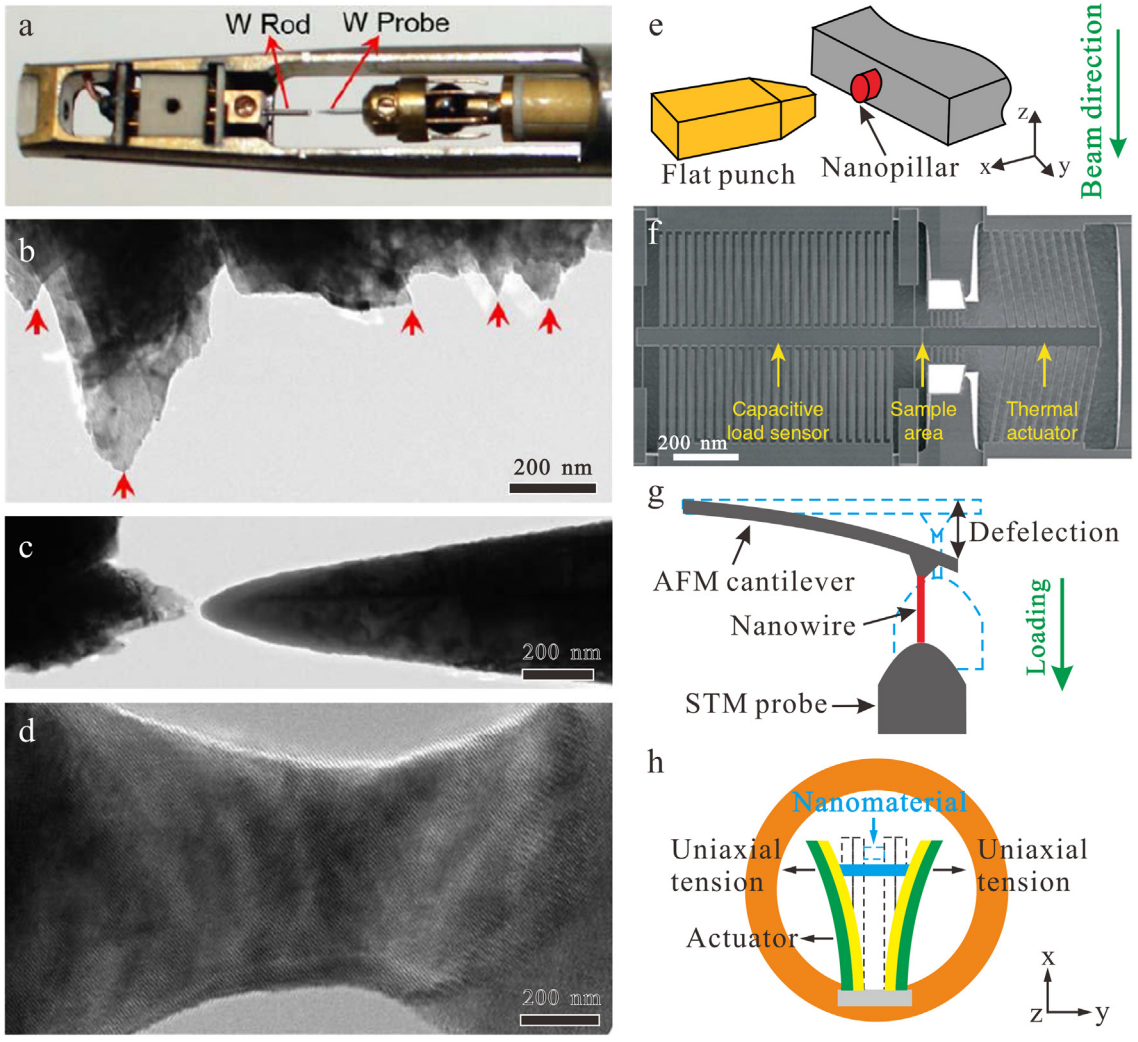

Fig. 1. TEM-based *in situ* nanomechanical testing methods. (a) The TEM–STM platform. (b) numerous metal nano-tips after cutting. (c) The two nanotips were driven to contact. (d) Bridge-shaped single crystal was generated after contacting. (e) Schematic of nanoindenter-based *in situ* TEM tensile testing. (f) The MEMS stage used for *in situ* TEM tensile testing. (g) Schematic of the AFM-STM tensile testing platform. (h) Schematic of the thermally actuated TEM tensile device.
Source: (a-d) reprinted with the permission from Ref. [37]. © 2015, Nature Publishing Group. (f) reprinted with the permission from Ref. [41]. © 2015, Nature Publishing Group.

between GB and twin boundary (TB) [56–58], or other pre-existing defects/interfaces [59,60]. In submicro/micro-sized face-centered-cubic (FCC) and body-centered-cubic (BCC) single crystals, the dominant dislocation nucleation mechanism changed from Frank–Read source to single-arm dislocation source, as reported by Chisholm et al. [61], Kiener et al. [62] and Oh et al. [63]. Due to the image attractions from free surfaces, dislocations escaped from crystal quickly before multiplying. The limited dislocation multiplication led to a 'dislocation starvation' state so that higher stress is required for activating new dislocation source with reduced source length to accommodate further plasticity, as confirmed by Shan et al. [31]. Thus, the deformation mechanism changed from forest-hardening model in bulk materials to source-controlled plasticity with sample dimensions decreasing [62,64]. Owing to the insufficiency of traditional dislocation source, single-arm source, truncated by free surface ('source truncation'), was operative in constrained crystal volume [65]. Given that the critical stress to activate single arm sources depends on the dislocation length, small-sized FCC metals follows a power-law scaling on crystal size with the power-law exponent of approximately −1. To the contrary, the plastic mechanism of sub-micron BCC crystals follows the classical model of forest-hardening more closely than the dislocation starvation model [66, 67]. Due to the easy cross slip of screw dislocations enhanced by the image stress, a dislocation cusp easily formed and resided inside crystals, which eventually develops into a loop. During mechanical loading, the dislocation arms propagated, through the crystal and then generated multiple dislocation segments [68,69]. Furthermore, a long residence lifetime for screw dislocations in BCC pillars enhances the probabilities of junction formation and forest dislocation interactions. Thus, the dominated deformation mechanism in BCC small-volume metals is similar to the forest-hardening model in bulk metals, and the strengthening power-law exponents is nearly −0.4 [70,71]. Kiener et al. [62], Uchic et al. [72] Greer et al. [70,73] and Mompioua et al. [64] demonstrated that the Hall–Petch-type strength-size dependence does not hold true only for nanocrystalline materials, but also for small-sized FCC and BCC single crystals.

As sample dimensions further decrease to nanoscale, the operation of single-arm dislocation sources give way to surface dislocation nucleation (SDN). Zheng et al. [13] directly observed surface dislocation nucleation process in sub-10-nm gold (Au) nanowires (NWs). As the lattice stress in the Au NW reached to a yielding point, a leading partial nucleated from a favorable surface step (Fig. 2a), propagated through crystal leaving behind a stacking fault (SF) as shown in Fig. 2b. Subsequently, a trailing

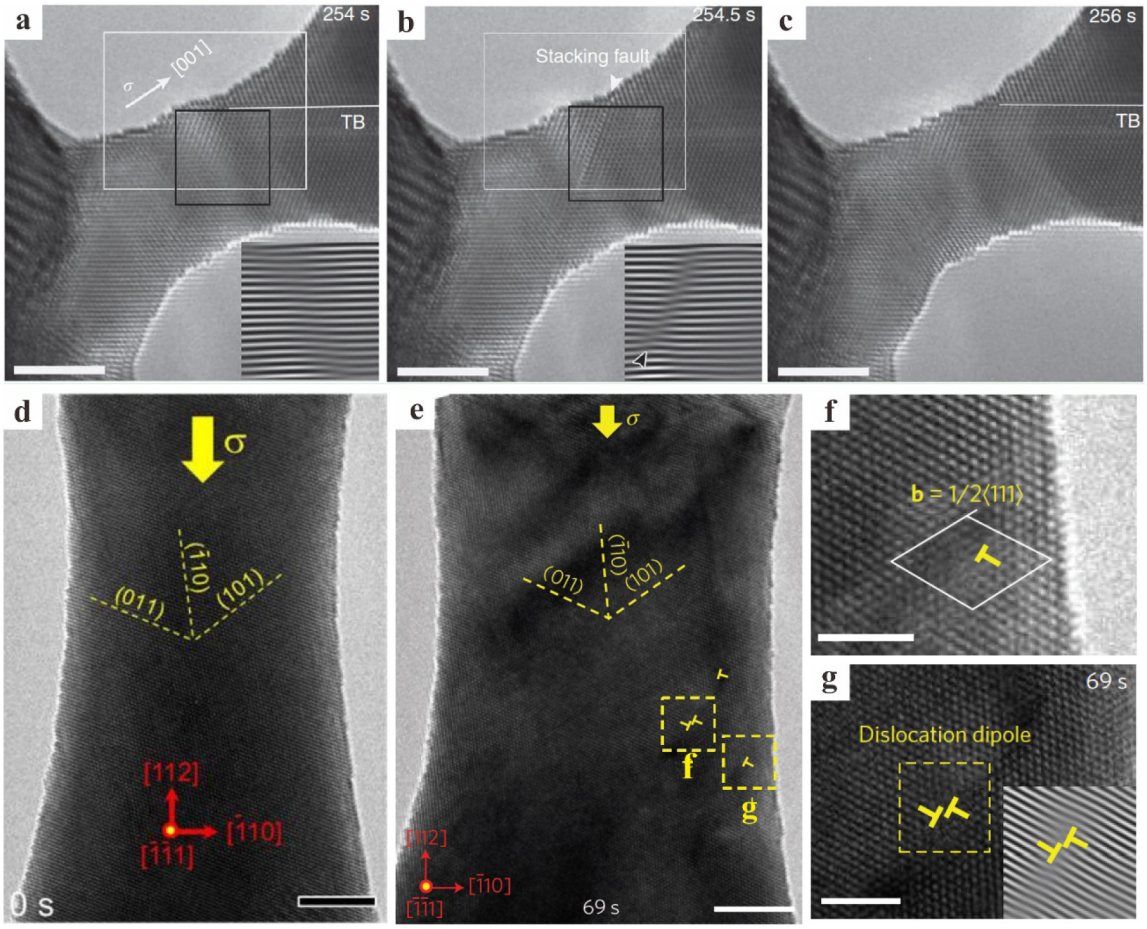

Fig. 2. Surface dislocation nucleation in metallic nanowires. (a-c) Sequential HRTEM images showing the entire process of dislocation dynamics. The insets in a and b are Fourier-filtered images of the black square area. The scale bars are 3 nm. (d-e) TEM images of dislocation dynamics in W NW. Scale bars in d-e are 5 nm. (f-g) TEM images of 1/2⟨111⟩-typed mixed dislocation nucleated from surface. Scale bars in f-g are 2 nm.
Source: (a-c) reprinted with the permission from Ref. [13]. © 2010, Nature Publishing Group. (d-g) reprinted with the permission from Ref. [37]. © 2015, Nature Publishing Group

partial nucleated, eliminated the SF, and then form a full dislocation, which glided through NW and annihilated at the opposite surface (Fig. 2c). The plasticity in Au NW is thus mediated by discrete dislocation nucleation and propagation. Besides, surface dislocation nucleation also serves as the prevalent deformation mode in nanosized metals with other crystal structures. Wang et al. [37,40] revealed the plasticity of BCC tungsten (W) nanowire under ⟨112⟩ compression is mediated by dislocation slip (Fig. 2d and e), including the nucleation of 1/2⟨111⟩-type mixed half dislocation loop from surface (Fig. 2f and g), subsequent dislocation glide on the {110} slip planes and the eventual escape of dislocations at surface. The dislocation nucleation behavior in W nanocrystals is affected by the deformation strain, with the favorable nucleation site changed from (110) surface to (111) surface with the increase in compressive strain. It was also revealed that local high strain concentration near the shear band interfaces catalyzes the nucleation of new dislocations causing discrete thickening of shear bands. Similar to FCC and BCC pristine single nanocrystals, SDN process also dominated plasticity in other nanostructured materials with the characteristic length scale of microstructure ranging from submicrometer scale to angstrom scale, such as nanotwinned Au NWs [15,22], pentatwined silver (Ag) NWs [23,41,74], bitwinned Ag NWs [75] and bicrystalline Ag NWs [76]. Not only the dislocation nucleation source but also the type of the nucleated dislocation is influenced by the characteristic length scale of the nanostructured metals such as gain size [46], film thickness [77] and sample dimension [49,78,79]. With decreasing microstructural feature size, the critical nucleation stress for perfect and partial dislocations increased differently due to their different Burgers vector. Consequently, partial dislocation activities dominate over full dislocation activities at small scale. The size dependent nucleation stress of perfect vs. partial dislocations arises the competition between ordinary dislocation plasticity and deformation twinning.

SDN process is generally believed to be highly sensitive to some intrinsic factors (e.g. sample size) and extrinsic factors (e.g. temperature and strain rate) [80]. Strong size-dependence of the yield stress was reported in Au NWs [81], while weak size dependence of nucleation strength was observed in Pd [82] and Ag NWs [36]. Such distinct difference in size dependence of strength may be attributed to the unusual softening behaviors resulted from surface diffusional events in Pd and Ag nanocrystals, which offsets the strengthening effects caused by size reduction [36,82]. Furthermore, according to transition state theory, SDN is a thermally activated process so that nucleation strength is expected to be strongly dependent on temperature. In the *in situ* TEM tensile tests of Pd NWs, Chen et al. [82] corroborated the predictions that nucleation is assisted by thermal fluctuations. Moreover, SDN is found to be strain rate-controlled, with the yield strength of bicrystalline Ag NWs increasing markedly with strain rate [76]. The investigations mentioned above offer insights into size-, temperature- and strain rate-dependent

SDN in nanostructured materials, however, the influence of surface step morphology and chemical passivation layer on SDN remains experimentally unclear. Given that the fabricated NWs with different surface conditions usually suffer from various service conditions in a practical application, a sound understanding of SDN could provide useful material design strategies for material reliability in M/NEMS device.

4. Twining-related plastic mechanism

Metal materials with nanoscale twins embedded usually exhibit excellent mechanical properties compared with their twin-free counterparts, which have attracted intensive research interest in the field of material science and engineering [56,57]. Accordingly, the twining-related plastic deformation mechanism has been the subject of ongoing discussions. The current insights into the atomic-scale deformation mechanisms related to twining heavily rely on the MD simulations limited by high stress and short time conditions [83,84]. Because of very few direct experimental observations, particular at the atomic level, it remains unclear whether the deformation models proposed based on computational results can be directly extrapolated to those under laboratory condition. A thorough understanding of twinning-related plastic mechanism are of importance for not only fundamental scientific aspect but also providing novel material design clues for small-sized metal materials used in electronic devices.

In FCC metals, deformation twins initiated and then thickened through layer-by-layer movement of twining partial dislocations emitted from free surface [13,81,86,87]. Until very recently, Wang et al. [85] revealed a new deformation twinning route operating in FCC nanocrystalline (NC) platinum (Pt) unlike the classical layer-by-layer twinning route. A nanotwin embryo is nucleated through the formation of two SFs separated by a single atomic layer (Fig. 3a-b), and the subsequent emission of a partial dislocation between the two previously formed SFs (Fig. 3c). Not only the nucleation of a nanotwin embryo but also the growth of the twins in nanostructured materials could proceed without following the traditional layer-by-layer fashion. Sun et al. [48] observed that partial dislocations nucleated randomly from the surface of the Ag NWs on non-neighboring {111} planes, leading to a high density of SFs and finally the formation of a single nanotwin (NT) (Fig. 3d–i). The atypical twining routes in nanostructured materials may be facilitated by GBs and free surface to bypass the high stacking-fault energy. Deformation twinning has been well documented in FCC nanomaterials, while only dislocation-mediated plasticity was mostly reported in bulk and small-scale BCC metals at room temperature [88–90]. By using *in situ* HRTEM testing, Wang et al. [37] firstly found that twinning became the dominant deformation mode in BCC W NWs under room temperature (Fig. 4). Under compression, a twin embryo nucleated from the intersection between GB and surface and then propagated laterally into the nanowire as well as thickened through sequential nucleation of twinning dislocations on consecutive twining planes. Such twinning-dominated deformation was also observed to occur in niobium (Nb) NWs [91].

The two major plastic deformation mechanisms in metals are deformation twinning and full dislocation slip, which compete with each other directly through dislocation processes operating on the same set of slip systems [1]. The deformation behavior in FCC metal in response to mechanical stress can be well predicted by calculating and comparing the resolved shear stress on the slip systems based on Schmid's laws [92]. Lee et al. [93], Cao et al. [51], Zheng et al. [13] and Roos et al. [94] demonstrated that whether twining or full dislocation slip is dominant under a specific loading orientation depends on the maximum value of the Schmid factor between the leading partial and trailing partial, due to the fact that the first step in both deformation modes is the nucleation of a leading partial dislocation. In contrast to FCC metals, there is a lack of general established criteria for determining activated deformation mode in BCC metals. However, the analysis of the resolved shear stress on twining and slip systems still play a key part in determining the dominant deformation mechanism as confirmed by Wang et al. [37] and Wei et al. [95]. In addition to loading orientation, the deformation mechanisms were found to be strongly dependent on characteristic length scale (e.g. gain size, film thickness and sample dimension). For instance, Yue et al. [96] demonstrated a crossover from full dislocation slip to deformation twining below a critical crystal size of Copper (Cu) NW, analogous to the size effect reported in Au thin films [77], nanowire [78] and nanowhiskers [97]. The size-dependence of full vs. partial dislocation activity is attributed to the difference in nucleation stress for full and partial dislocation, that increase differently with decreasing microstructural feature size [78,97]. Moreover, the critical transition size is inversely proportional to stable stacking fault energy. Characteristic microstructural dimensions, stacking fault energy and loading orientation are generally believed to influence deformation mechanisms, however, Yin et al. [34] recently reported that cross-sectional shape of Ag NW, an additional factor, could affect the deformation mechanism in operation by influencing twining energy barrier, which is correlated with the surface energy change upon loading.

Dislocation–twin interactions play a fundamental role in the strengthening, strain-hardening and plasticity of metal materials containing TBs [98]. The introduction of nanoscale twins in bulk metals and small-sized metallic crystals has been demonstrated to be an effective method to enhance their mechanical properties (e.g. ultrahigh strength and high ductility), which has been a subject of long-standing interest to materials scientists [99]. Jang et al. [100] reported that the strength of nanotwinned Cu pillars with twin boundaries spaced at 4.3 nm reached nearly 40% of the ideal strength of Cu, 1.5 times higher than those of their twin-free counterpart, which is associated with the intrinsic brittleness of twin boundaries. Wang et al. [15,22] revealed that the strength of nanotwinned Au NWs increased with the reduction in twin spacing, and it reached near-ideal strength limit as the twin thicknesses decreased to an angstrom scale exhibiting a significant Hall–Petch-type strengthening behavior, which is attributed to the twin size-dependent deformation mechanism transition from heterogeneous dislocation nucleation from surface to homogeneous dislocation nucleation inside NWs. Moreover, TBs in Au NWs were found to act as barriers for slip transfer of partial dislocation, contributing to the observed strengthening and strain-hardening effects. Such blocking effect of TB on full and partial dislocations were also observed to occur in twin-structured nanocrystalline (NC) Pt during mechanical loading [83,84]. t is demonstrated that nanotwinned FCC metals reach the maximum strength at a specific size ratio of twin thickness to grain size, below which strengthening and strain hardening caused by dislocation twin boundary interactions occurs, whereas above the specific size ratio softening caused by detwinning is dominant [101]. In addition to the significant strengthening effect induced by TBs, twinning-related mechanism have been frequently observed to contribute to considerable plasticity in small-sized metals. Seo et al. [81,86] reported that coherent twin boundary (CTB) migration during mechanical loading reorients the lattice of the Au NW from ⟨110⟩ to ⟨100⟩ crystallographic direction, contributing to the high ductility of ∼50%. Thus, a good combination of ultrahigh strength and considerable ductility are achieved in Au NWs caused by size effect and long-ranged CTB propagation. Furthermore, a recent *in situ* TEM study on twin-structured Pt

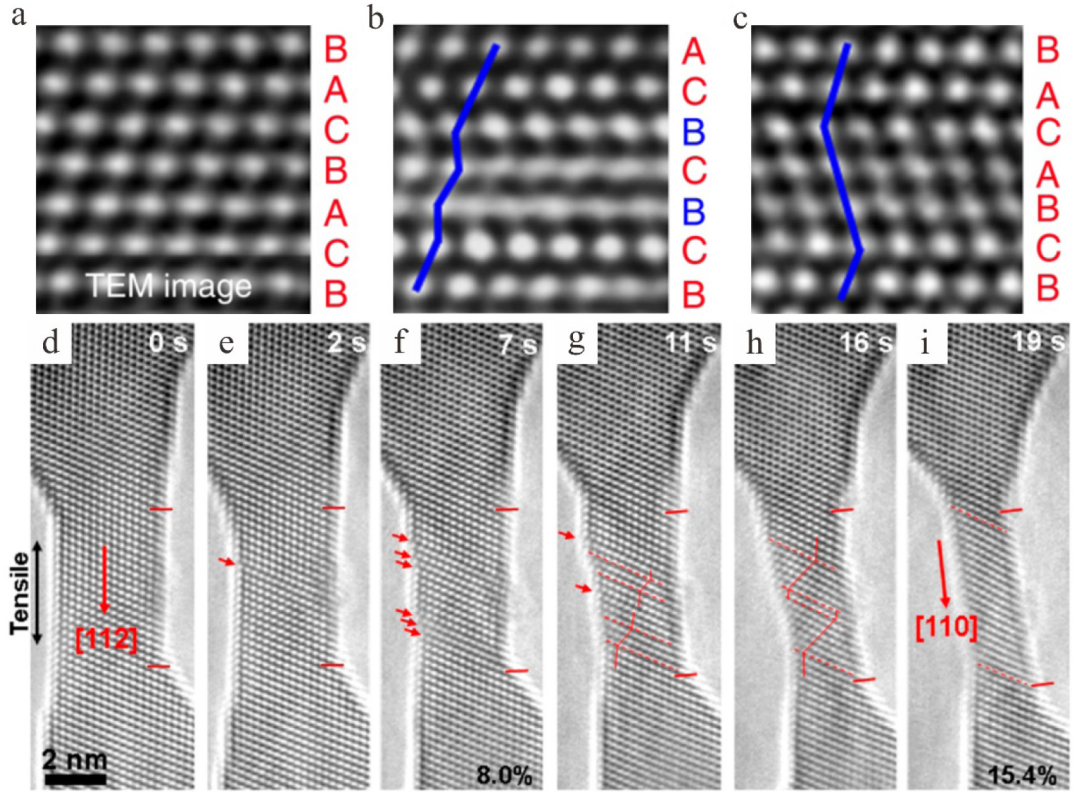

Fig. 3. Deformation twinning in FCC nanostructured materials. (a-c) HRTEM images and associated schematic illustrations showing the dynamical process of the nucleation of a three-layer twin. The scale bars are 1 nm. (d-i) A sequence of HRTEM images showing the formation of a nanotwin.
Source: (a-c) reprinted with the permission from Ref. [85]. © 2017, Nature Publishing Group. (d-i) reprinted with the permission from Ref. [48]. © 2019, American Chemical Society.

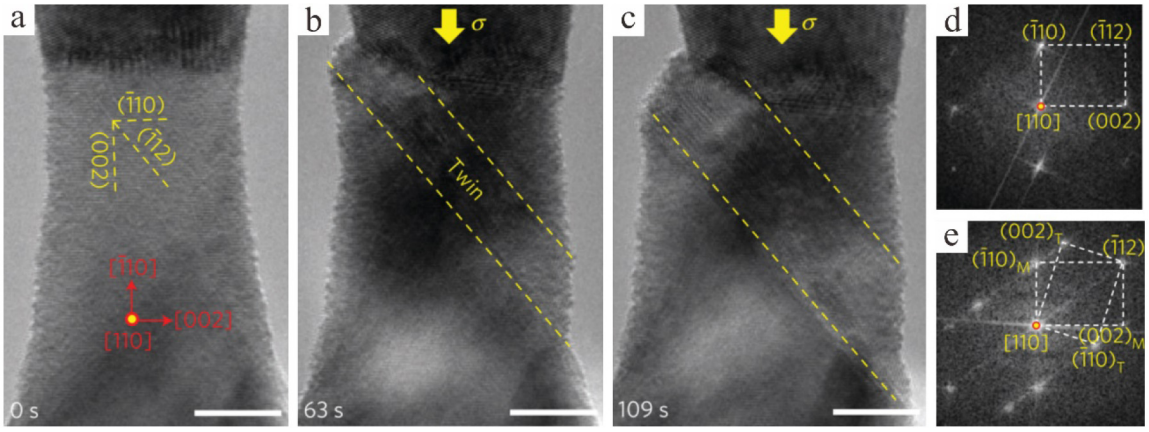

Fig. 4. Twinning-dominated deformation in BCC W metallic NWs. (a-c) Sequential HRTEM images showing the twinning process. The scale bar in each figure is 5 nm. (d-e) Fast-Fourier transformed (FFT) patterns of the original W NW and the deformation twinning, respectively.
Source: (a-e) reprinted with the permission from Ref. [37]. © 2015, Nature Publishing Group.

nanocrystals showed that incoherent twin boundary (ITB) migration also play a dominant role in the plastic deformation [83]. The migration of ITBs could proceed through the collective glide of multiple Shockley partial dislocations on every {111} plane that consist of ITB [102]. Besides, they directly observed that dislocation nucleation from TBs, the motion of dislocations intersecting with TBs, the interaction between TBs and dislocations, and CTB migration contribute to large plastic strain. Apart from the contribution of mechanical twinning to plastic deformation, TB assisted dislocation slip also contributed to plastic deformation. Fu et al. [103] found that the intersectional twins, a pathway for easy glide of dislocations, facilitate massive cross slips of dislocations from one TB to another, resulting in homogeneous deformation. Moreover, Wang et al. [104] revealed that surface nucleation of screw dislocations, subsequent slip transmission across TB, cross slip and final transition to a 60° dislocation contributed to the GB formation in the bent nanotwinned nickel (Ni) NW. Besides, detwinning mechanism also contributed to large plastic deformation, as revealed by Cheng et al. [75] in bitwinned Ag NWs with small volume ratios. Multiple dislocation nucleated from surface intersected and interacted with the preexisting TB resulting in the detwinning of a segment of the TB, which transit bitwinned phase into single crystal phase. A wealth of investigations has placed emphasis on the mechanical behaviors of twin-structured

nanomaterials; however, atomistic understanding of twinning-related plastic mechanism is still lacking and thus requires to be studied further, considering the huge potential of small-sized metals with nanoscale twins in a practical application.

5. Phase transformation in nanocrystals

Due to the constrained volume of nanocrystals, ordinary full dislocation slip and deformation twining may be suppressed due to the high critical shear stresses needed to nucleate a perfect dislocation and partial dislocation. In this case, alternative plastic deformation mechanisms, such as phase transformation, may be activated in small-volume metallic crystals. MD simulations predicted that NWs could undergo phase transformation driven by surface stresses and the tendency to minimize surface energy [105,106]. The accuracy of MD simulations, however, are usually limited by the empirical interatomic potentials such that the computational results are inconsistent with each other [1,105,107]. *In situ* HRTEM testing technique is thus utilized to provide unambiguous experimental evidence for the atomic-scale deformation process of phase change in nanometer-scale materials. Advances in understanding of the phase stability and transformation from a fundamental perspective may provide new clues for optimizing microstructures and thus improving the mechanical properties of metal materials.

In situ HRTEM mechanical tests have demonstrated that phase transformation from FCC to body-centered tetragonal (BCT) could occur to accommodate the plasticity of FCC nanocrystals. For instance, Zheng et al. [13] reported that the Au NWs underwent phase transition spontaneously under zero applied load (Fig. 5a-g). Since the compressive stresses inside Au NWs induced by surface effect are inversely proportional to the crystal size, after the fracture of Au NW, the compressive stresses inside the NW, that were large enough to overcome the energy barriers for martensitic transition, led to the structure relaxation through the contraction of the NW along ⟨001⟩ crystallographic direction and the formation of new BCT phase following Bain path. The phase transformation from FCC to BCT was also reported under bending condition, as confirmed by Wang et al. [108]. Bending deformation of nickel (Ni) NW induced a continuous lattice strain along the axial direction such that the inter-plane lattice angle of the {111} planes changed continuously from 70.5° in an original FCC structure to 90° in a BCT structure and finally to 109° in a re-oriented FCC structure, resulting in a ultralarge shear strain of 34.6%. Different from the classical phase transformation path, martensitic transformation and Bain transformation, the phase transition from FCC to BCT during bending was associated with the lattice shear in the ⟨112⟩ {111} system. In addition to FCC NWs, phase transformation was also observed to mediate the plasticity of nanostructured materials with other crystallographic structure.

For BCC nanostructured materials, Wang et al. [91] directly observed that deformation-induced phase transformation resulted in significant crystallographic reorientation contributing to large plasticity in niobium (Nb) NWs. Upon tension, ultrahigh shear stress in the shear band provided a driving force for phase transition from an initial [100]-oriented BCC structure to a metastable [110]-oriented FCC phase with higher energy (Fig. 5h-i). The orientation relations between these two phases were $[100]_{BCC}//[011]_{FCC}$ and $(01\bar{1})_{BCC}//(1\bar{1}1)_{FCC}$, following the Nishiyama–Wassermann (N-W) relationship [109]. With further loading, the newly formed phase boundaries extended gradually along the length direction, and then the FCC phase transformed to a [111]-oriented BCC lattice rapidly with the orientation relations between these two phases following the Kurdjumov–Sachs (K-S) relation ($[011]_{FCC}//[111]_{BCC}$ and $(1\bar{1}1)_{FCC}//(01\bar{1})_{BCC}$), as shown in Fig. 5j [110]. Consequently, the plastic deformation of Nb NWs proceeded continuously through the two-step BCC–FCC–BCC phase transformation with an FCC phase being an intermediate phase (Fig. 5k). The uncovered phase transformation from BCC phase to metastable FCC phase followed the Bain lattice deformation process, traditionally used to model a martensitic transformation from an FCC structure to a BCC structure [111]. Such kind of two sequential structural transformations coupled with shear deformation were also observed to occur in the region ahead of a crack tip in BCC molybdenum (Mo) thin film, as revealed by Wang et al. [112]. It was also revealed that the newly formed [111]-oriented BCC lattice and [110]-oriented FCC lattice transformed back to the initial BCC structure upon unloading the imposed stresses.

Thus far, all the experimental evidences on phase transformation in nanostructured materials were based on a single two-dimensional image along a specific zone axis (e.g. ⟨110⟩ in FCC and ⟨100⟩ in BCC); However, from a basic science point of view, determining a new phase with a specific crystallographic structure requires HRTEM images along at least two zone axes, which is technically demanding to be studied by the current *in situ* HRTEM techniques. Considering that *in situ* HRTEM tests on nanostructured materials provide atomic-scale information on solid-state transformations not easily ascertained in bulk solids, advanced experimental techniques are thus needed to be developed in the future to provide ample information on structural transformation. From an application standpoint, phase transformation causes fundamental changes in the structure and may dramatically influence the mechanical properties of metals. A thorough understanding of deformation-induced phase transformation is of prime importance for the mechanical stability of small-volume metals used in electronic devices.

6. Diffusion-mediated plastic deformation

Substantial surface area to volume ratio is one of the characteristics of small-sized metallic materials with a large proportion of the constituent atoms residing on free surfaces [80,113,114]. The surface atoms are under-coordinated and tend to reduce surface energies, creating a tensile surface stress, that is inversely proportional to the crystal size [115–118]. Moreover, free surfaces in nanostructured materials, similar to the roles of GBs in NC metals, could act as a highway for mass transport [119–121]. As the crystal size goes down to a characteristic length scale, ultrahigh surface stress could break surface atomic bonds and subsequently gives rise to diffusional mass flow along free surfaces, which severely threatens the long-term shape stability of nanosized materials [122]. In a practical application of nanometals widely used in electronic devices, precise shape control of components is of vital importance. Deep insights into diffusional plasticity at atomic scale is therefore essential for the reliability and stability of nano-structured devices.

Displacive and diffusional deformation are generally viewed as two major competing modes of plastic deformation in nanoscale materials. Displacive deformations govern plasticity at room temperature, while diffusional plasticity often occurs at high temperature [124–126]. Aside from the temperature, size scale can be a decisive factor on the operative deformation mechanism during mechanical loading. At very small crystal sizes in the range of a few nanometers, diffusional deformation should be the only carrier of plasticity for nanoscale materials, and this is especially true for some metals that have a relatively low melting temperature [127]. Sun et al. [122] found that sub-10 nm Ag nanoparticles was deformed like a liquid droplet (namely, a reversible change in shape) but kept crystalline character in the interior without observable displacive plasticity and lattice structure evolution

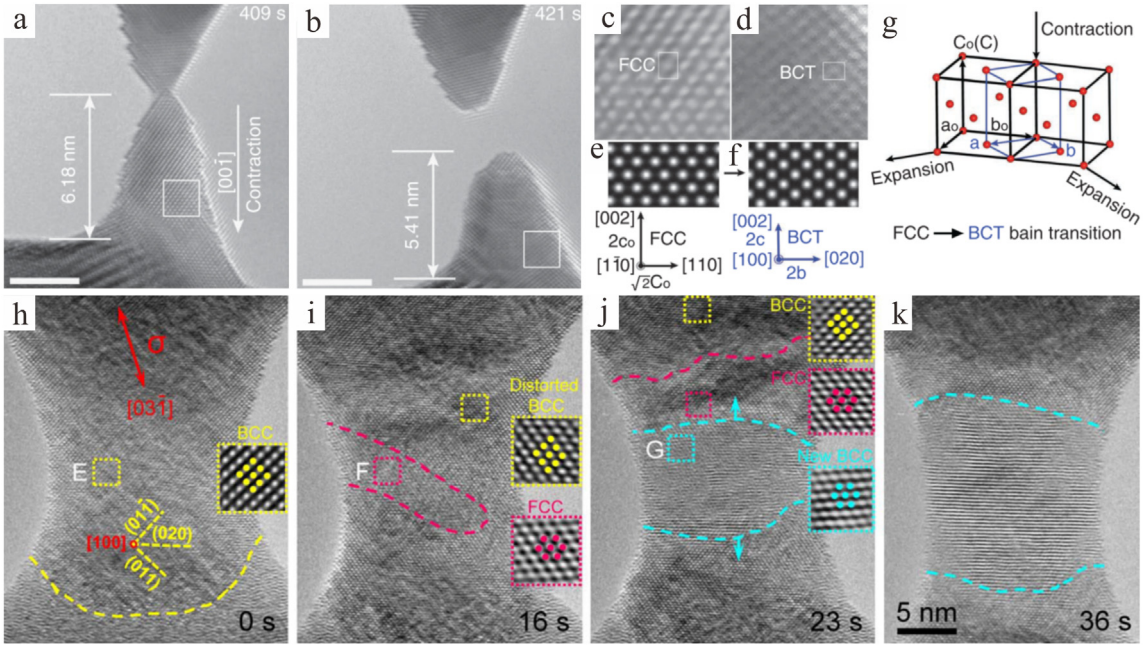

Fig. 5. Phase transformation in metallic nanocrystals. (a-b) HRTEM images of the Au NW before and after fracture. The scale bar is 3 nm. (c-d) Enlarged images of the white-boxed area in a and b, respectively. (e-f) Simulated HRTEM images of FCC-Au with lattice parameter of a = 4.078 Å along [110] zone axis and BCT-Au with a = b = 3.34 Å and = 2.86 Å along [100] zone axis, respectively. (g) Phase transformation from FCC to BCT through the Bain path, attributed to the lattice distortion along [001] direction in FCC crystal. The unit cells of FCC and BCT lattice structure were labeled out by black and blue lines, respectively. (h) Pristine Nb NW aligned in the [100] zone axis. (i) The initial BCC lattice transformed to a [110]-oriented FCC lattice. (j) Phase transition from an intermediate FCC lattice to a [111]-oriented BCC lattice. (k) Sequential phase transition followed a BCC–FCC–BCC pathway. The pink and cyan dashed lines represent phase boundaries. . (For interpretation of the references to color in this figure legend, the reader is referred to the web version of this article.)
Source: (a-g) reprinted with the permission from Ref. [13]. © 2010, Nature Publishing Group. (h-k) reprinted with the permission from Ref. [91]. © 2018, Science Publishing Group.

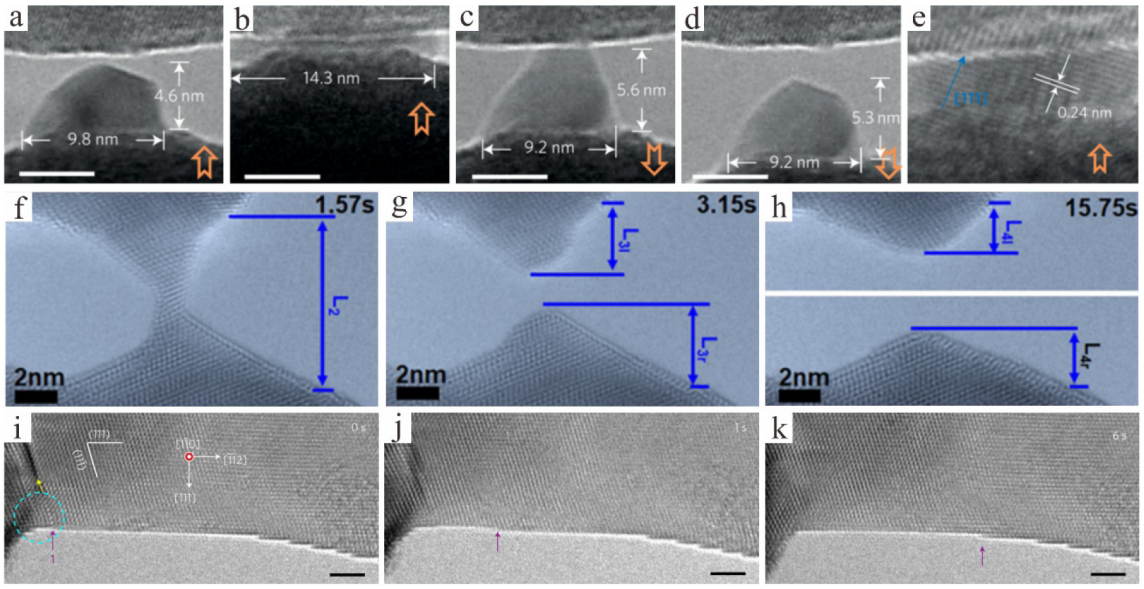

Fig. 6. Diffusion-mediated deformation in FCC nanostructured materials. (a-d) Sequential HRTEM images showing the liquid-like pseudoelastic deformation of the Ag nanocrystal. The scale bars are 5 nm. (e) A snapshot of the Ag NC during deformation. The crystal remained highly crystalline in the interior during deformation. The scale bar is 5 nm. (f-h) Atomic-scale images of contraction process of an Au NW mediated by surface atom diffusion. (i-k) Slip-activated surface diffusional deformation in Ag NW.
Source: (a-e) reprinted with the permission from Ref. [122]. © 2014, Nature Publishing Group. (f-h) reprinted with the permission from Ref. [123]. © 2018, American Chemical Society. (i-k) reprinted with the permission from Ref. [36]. © 2017, Nature Publishing Group.

during cyclic compression and stretching (Fig. 6a-e). The liquid-like pseudoelasticity is associated with the geometry reconstruction of Ag nanocrystal that is mediated by surface atom diffusion driven by capillary-energy minimization. Furthermore, a wealth of *in situ* TEM tensile tests of Cu, Ag and Au NWs revealed that the liquid-like deformation behavior occurred frequently after the fracture of NWs [36,122,123,128–130]. When the fracture happened, atom diffusion processes at free surfaces with high curvatures were highly active such that the locations of large curvatures continuously smoothed out, and at the same time the

fractured tips retracted rapidly with length reduction and diameter expansion (Fig. 6f-h). Consequently, diffusional deformation played a critical role in the contribution of ultralarge contraction strain of the fractured NWs, and resulted in the rounded and smooth shape of the fractured tips finally. Moreover, along with the deformation mechanism transition from displacive to diffusional deformation, the strength-size relationship changed from Hall–Petch-like 'smaller is stronger' tend to 'smaller is much weaker' diffusion softening regime, as demonstrated by the *in situ* TEM deformation tests of Tin (Sn) samples [119].

Not only a competition relationship but also a cooperative interplay between diffusional creep and crystal slip existed in FCC NWs, as demonstrated by *in situ* HRTEM straining tests. Zhong et al. [36] revealed that coupled diffusive-displacive process replaced pure crystal slip or diffusional creep as the dominant deformation mechanism, contributing to room-temperature superplasticity in Ag NWs within a critical size regime. Crystal slip, serving as a stimulus to surface diffusional creep, generated atomic-scale steps with one atomic layer at free surface (Fig. 6i). Such abrupt change in surface morphology resulted in that the chemical potentials of the atoms at surface steps were much higher than those elsewhere. To lower the overall system energy, significant curvature- and stress-driven diffusional deformation occurred via continuous lateral movements of the surface atoms at step edges (Fig. 6j-k), giving rise to a self-healing mechanism that maintained a relatively smooth surface contour, and thus prevented shear localization and the tendency of plastic instability during mechanical loading. In addition, Sun et al. [48] found that a partial dislocation slip promoted surface atom diffusion by introducing a surface step with a height of one-third of an atomic-layer, that have a low coordination number favoring atom diffusion. They also found that the partial dislocation-induced surface steps cannot be eliminated by surface atom diffusion, and thus constantly serve as a preferred site for the initiation of new surface atom diffusion events during mechanical loading. Different from the large-scale and long-distance surface atom diffusion stimulated by crystal slip, displacive plasticity is influenced by localized diffusion of surface atoms in Au NWs [51]. Surface diffusion of individual atoms occurred occasionally and then smoothed surface uniformity, changing the height and length of surface steps. Such change in local surface morphology alleviated high strain concentration at the dislocation-induced surface steps, therefore eliminating the possibility of dislocation nucleation and subsequent deformation localization from the same surface site.

MD simulations have been proved to be an effective method to investigate mechanical deformation mechanisms at atomic scale. However, due to the extremely high strain rate and the very short-lived simulation time (less than a nanosecond), diffusion-mediated plasticity in MD simulations is not obvious unless at elevated temperature compared to experimental results [131, 132]. It leads to some difficulties when extrapolating from the computational results to those under laboratory conditions. Although various of diffusional deformation mechanisms have been proposed by *in situ* TEM tests, the validity of these mechanisms remains questionable. For instance, Zhong et al. [36] predicted that pure diffusional creep governed plasticity in Ag NWs with sample diameters less than 15 nm. Moreover, Sun et al. [122] found that the plasticity of sub-10 nm Ag nanocrystals was fully controlled by surface atom diffusion. In contrast, Sun et al. [48] observed that the dislocations were still active in the plastic deformation processes of sub-5 nm Ag NWs. Considering the inconsistencies reported in previous papers, more experimental efforts should be made in revealing a more general theory on diffusional deformation mechanisms to advance our basic knowledge of plastic deformation behaviors in small-sized metals.

7. Reversible structure transition-induced pseudoelasticity

Both plastic and pseudoelastic deformations are associated with structure change in response to mechanical loading, resulting in energy dissipation [1]. The essential difference between them, however, is that most plastic strain is reversible in the pseudoelastic effect. As soon as the applied load is removed, a deformed sample always recovers to its original shape completely regardless of previous deformation history, whereas a component deformed by plasticity stay in the deformed shapes at zero stress, and requires imposing a negative load to recover its original shape [122]. Pseudoelasticity and shape memory effects, mediated by martensite phase transformation and reversible movement of TBs, were frequently observed in bulk shape memory alloys [133,134]. Due to their important applications in coupling, sensing, and actuation, shape memory alloys have attracted significant interest from scientific and industrial research. Until recently, a wealth of experimental observations and MD simulations revealed that pseudoelasticity could also be achieved in single-crystalline nanostructured materials due to its peculiar structure different from their bulk counterparts [135–140]. All the plastic deformation mechanisms mentioned in the previous sections, such as displacive deformation, phase transformation, diffusional plasticity, give rise to the possibility of reversible structure transition process causing pseudoelasticity in small-sized metal materials.

Free surface in nanostructured materials played an important role in mediating reversible plastic deformation. For instance, Zheng et al. [141] found that surface-mediated dislocation activity resulted in recoverable plasticity in Au NWs. During mechanical loading, the dislocations, nucleated from free surface, piled up and formed a low angle grain boundary (LAGB) inside the NW (Fig. 7a). After the removal of external stress, the dislocations were completely annihilated at free surfaces driven by back force from dislocation pile-up and image force from free surfaces. Concurrently, the newly formed LAGB suddenly vanished, causing reversible plastic strain, that is, pseudoelasticity (Fig. 7b). The fully reversible plastic behavior mediated by dislocation activities was also observed by *in situ* tensile tests of penta-twinned Ag NWs [41]. During loading step, dislocation nucleated from surface, propagated inside the NW and terminated at TBs (Fig. 7c-d). In the course of unloading deformation, the dislocations retracted and disappeared causing that the deformed NW was totally recovered (Fig. 7e-f). Given that surface image force exerted on dislocation is inversely proportional to crystal size, such surface-mediated recoverable plasticity can only occur in nanoscale materials [141]. In addition to dislocation nucleation and annihilation sites, free surface in nanocrystals could act as a highway for atom diffusion. Diffusion of surface atoms mediated pseudoelastic deformation in Ag nanocrystals leading to a liquid-like recoverable shape change [122].

Reversible lattice reorientation process also gives rise to pseudoelasticity in small-sized metallic materials. As discussed in the previous phase transformation section, under continuous lattice shear strain, a reversible and continuous phase transformation occurred in Ni NWs, where lattice changed from a FCC structure to a BCT structure and finally to a re-oriented FCC structure [108]. Furthermore, a BCC–FCC–BCC phase transformation induced by shear stress was observed to be reversible in BCC Mo materials during loading and unloading [112]. Aside from phase transformation, consecutive twining and detwinning process is another mechanism of lattice reorientation that cause reversible plastic deformation, as demonstrated by Lee et al. [93]. Under tensile loading, [110]-oriented Au NW deformed by deformation twinning leaving behind nano-scale twins in Au NW. When the twinned NW was subsequently compressed, the twins shrank

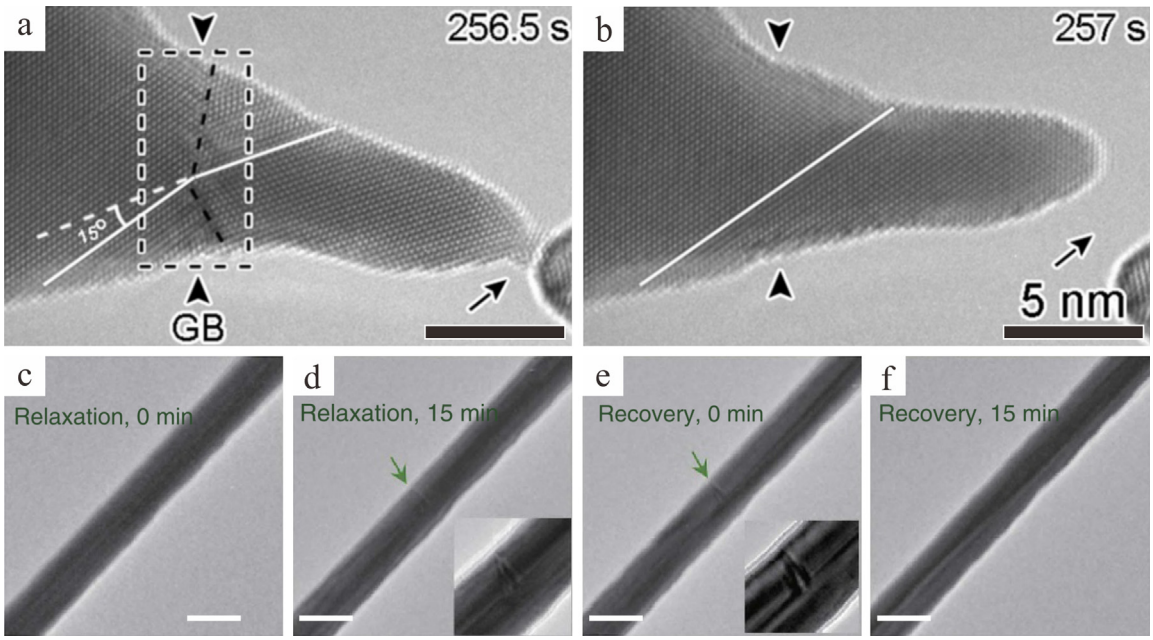

Fig. 7. Surface-mediated pseudoelasticity in FCC NWs. (a) Dislocation pile-ups result in the formation of LAGB in the Au NW. (b) LAGB disappeared during unloading step. (c-f) A series of TEM images showing dislocation nucleation, termination at TBs and annihilation in a penta-twinned Ag NW. The scale bars are 150 nm. *Source:* (a-b) reprinted with the permission from Ref. [141]. © 2012, American Physical Society. (c-f) reprinted with the permission from Ref. [41]. © 2015, Nature Publishing Group.

continuously and disappeared eventually. Reversible twinning and detwinning process under cyclic tension and compression is a direct consequence of the interchange in Schmid factor between the leading and trailing partial dislocations. Schmid factor favored a trailing dislocation over a leading dislocation during compression such that trailing partials annihilate the stacking fault on the preexisting twin boundary causing detwinning process. Li et al. [142,143] directly observed twinning and spontaneous detwinning at the crack tip of aluminum (Al) and Ni. Since the stacking fault energy (SFE) is high and the lattice friction force against the detwinning partial dislocations is relatively low for Al and Ni, the stacking fault force and surface image force during unloading are large enough to drive detwinning process to reduce system energy. Furthermore, mobile Shockley partials on ITBs can migrate under external stress and lead to the migration of TBs. Deformation twinning in BCC NWs is also pseudoelastic, as demonstrated by Wang et al. [37]. During loading and unloading cycles, twining and detwinning process proceeds through the nucleation and propagation of twinning dislocations in a layer-by-layer fashion, but in the reverse direction. The detwinning process during unloading was attributed to back stress resulted from strain incompatibility at the intersection between GB and TB [144, 145]. Until very recently, Wang et al. [146] found that the high interface energy of inclined TBs and surface image force provided driving force to detwinning process in twinned W nanocrystals causing pseudoelasticity.

The pseudoelastic deformation mechanisms mentioned above offer new insights towards the understanding of the mechanical properties of the small-sized metallic materials with FCC and BCC structures. Yet, the critical length scale and temperature for activating reversible plastic deformation in different classes of metals remain unknown. Further *in situ* experimental studies at atomic scale are needed to investigate pseudoelastic behaviors in small-volume systematically. Given the capability of recovering large inelastic strains and the low production costs compared with shape memory alloys, single-crystalline nanostructured material is a prominent candidate for the next generation of safer and more reliable nanodevices.

8. Summary and outlook

In summary, atomistic experimental mechanics open up a new opportunity for gaining deep insights into mechanical behaviors of small-sized materials at atomic scale. We have reviewed four most common deformation modes in small-sized metals, including ordinary dislocation slip, deformation twinning, phase transformation and diffusional deformation, which usually compete or couple with each other. The competition between deformation mechanisms under mechanical loading has been shown to be highly sensitive to some intrinsic factors (e.g. characteristic length scale, lattice structure, geometry, pre-existing defects and surface morphologies) and several extrinsic factors (e.g. strain rate, loading orientation, and temperature). Free surface in nanostructured materials play a crucial role in mediating plasticity. As a defect nucleation and annihilation site, free surface is a major cause of the size dependence of yield strength, achieving superior mechanical performances in small-volume metals over their bulk counterparts. Besides, ultrahigh stress appeared at free surfaces, causing phase transformation in metallic nanocrystals. Moreover, free surface is also a pathway for atom diffusion, probably giving rise to surface atom diffusion in response to mechanical loading. Although the mechanical behaviors of small-sized metals have attracted intensive research interest, the recent studies only focus on the deformation mechanisms of several materials under uniaxial loading conditions, that is merely a very small part of what actually happened in a practical application. A thorough understanding of the mechanical properties in small-volume materials is of vital importance for not only realizing their potential applications in the next generation nanodevices but also establishing a complete structure—property–deformation map of nanostructured materials. Thus, some future directions for research are enumerated as follows.

1. Until now, numerous theoretical and experimental investigations have been conducted to study the mechanical behaviors of small-sized metals under uniaxial loading at room temperature. Instead, mechanical behaviors under other loading modes (such

as bending and torsion) at elevated temperature has been less studied due to technical difficulties. Advanced testing methods capable of applying complex loading and controlling temperature concisely are thus in urgent need to investigate atomistic mechanical behaviors of small-sized materials systematically. Since the actual working conditions for small-sized metals are often more complicated than those under laboratory conditions, deep insights into atomic-scale deformation mechanisms under different loading conditions could provide new guidelines for designing new nanostructured metals with excellent mechanical performance.

2. It has been well accepted that when the layer thickness in metallic multilayered composites decreased from sub-microns to few nanometers, the operative deformation mechanism changed from a dislocation pile-up-based Hall–Petch model to confined layer slip of single dislocations and finally to an interface cutting mechanism [147–150]. By using *in situ* TEM test, Li et al. [151] directly observed that confined layer slip was the dominant deformation mechanism in a 30 nm Cu/20 nm Nb multilayer film. Thus far, direct experimental evidence for the interface cutting mechanism is still lacking due to the difficulty in fabricating *in situ* multilayered composites with individual layer thickness smaller than 2 nm. Further studies are still needed to provide deep insights into deformation mechanisms of multilayered composites unambiguously.

3. GB motion under stress plays a significant role in many processes, including grain growth, recrystallization, phase transformation and plasticity [27,152–154]. The migration mechanisms of LAGB, TB and ITB have been well documented, while the underlying mechanism of high-angle GB (HAGB) migration are still in their relatively infancy because of the complexity of HAGB migration [155]. *In situ* TEM nanomechanical test provides a unique opportunity to visualize the dynamic process of GB migration, that may reveal new atomistic mechanism of GB migration, leading to solutions of many longstanding puzzles.

4. Alloys, such as twinning-induced plasticity (TWIP) steels and high-entropy alloys (HEAs) has been found to display high strength with substantial uniform ductility, which have drawn significant attention [156–158]. Advanced energy-dispersive spectroscopy (EDS) in TEM are capable to probe chemical element distribution in alloys at atomic scale [159,160]. Combining advanced element recognition techniques with *in situ* mechanical testing platform is a promising way to gain a deep insight into the composition–structure–property relationships, that may provide new clues for tuning composition to produce outstanding mechanical properties in alloys.

5. Since *in situ* TEM nanomechanical tests were usually conducted in vacuum chambers, the effects of environment on the mechanical properties of NWs were usually excluded. However, in actual service conditions, the metallic NWs were often deformed under an oxidation environment. The underlying mechanisms describing the influence of oxidation on the mechanical properties remain largely unexplored [161,162]. Thus, quantitative *in situ* mechanical testing platform combined with gas environmental TEM is needed to be developed in the future, which can provide crucial clues for predicting the mechanical performances of small-sized materials in their practical application environments.

CRediT authorship contribution statement

Sixue Zheng: Wrote and revised the paper. **Scott X. Mao:** Wrote and revised the paper.

Declaration of competing interest

The authors declare that they have no known competing financial interests or personal relationships that could have appeared to influence the work reported in this paper.

Acknowledgment

S.X.M. acknowledges support from the NSF 1760916 through University of Pittsburgh.

References

[1] C.R. Weinberger, W. Cai, Plasticity of metal nanowires, J. Mater. Chem. 22 (8) (2012) 3277–3292.
[2] D.J. Fonseca, M. Sequera, On MEMS reliability and failure mechanisms, Int. J. Qual. Stat. Reliab. 2011 (2011).
[3] B.E. Alaca, J.C. Selby, M. Saif, H. Sehitoglu, Biaxial testing of nanoscale films on compliant substrates: Fatigue and fracture, Rev. Sci. Instrum. 73 (8) (2002) 2963–2970.
[4] C. Wang, D. Hwang, Z.B. Yu, K. Takei, J. Park, T. Chen, B.W. Ma, A. Javey, User-interactive electronic skin for instantaneous pressure visualization, Nature Mater. 12 (10) (2013) 899–904.
[5] S. Wagner, S.P. Lacour, J. Jones, P.H.I. Hsu, J.C. Sturm, T. Li, Z.G. Suo, Electronic skin: architecture and components, Physica E 25 (2–3) (2004) 326–334.
[6] S.X. Zheng, X.M. Luo, D. Wang, G.P. Zhang, A novel evaluation strategy for fatigue reliability of flexible nanoscale films, Mater. Res. Express 5 (3) (2018) 035012.
[7] R. Hofbeck, K. Hausmann, B. Ilschner, H.U. Kunzi, Fatigue of very Thin Copper and Gold Wires, Scr. Metall. Mater. 20 (11) (1986) 1601–1605.
[8] B.J. Kim, H.A.S. Shin, J.H. Lee, T.Y. Yang, T. Haas, P. Gruber, I.S. Choi, O. Kraft, Y.C. Joo, Effect of film thickness on the stretchability and fatigue resistance of Cu films on polymer substrates, J. Mater. Res. 29 (23) (2014) 2827–2834.
[9] S.X. Zheng, X.M. Luo, G.P. Zhang, Cumulative shear strain–induced preferential orientation during abnormal grain growth near fatigue crack tips of nanocrystalline Au films, J. Mater. Res. (2020) 1–8.
[10] T. Zhu, J. Li, A. Samanta, A. Leach, K. Gall, Temperature and strain-rate dependence of surface dislocation nucleation, Phys. Rev. Lett. 100 (2) (2008) 025502.
[11] Y. Fan, Y.N. Osetsky, S. Yip, B. Yildiz, Onset mechanism of strain-rate-induced flow stress upturn, Phys. Rev. Lett. 109 (13) (2012) 135503.
[12] C. Deng, F. Sansoz, Fundamental differences in the plasticity of periodically twinned nanowires in Au, Ag, Al, Cu, Pb and Ni, Acta Mater. 57 (20) (2009) 6090–6101.
[13] H. Zheng, A. Cao, C.R. Weinberger, J.Y. Huang, K. Du, J. Wang, Y. Ma, Y. Xia, S.X. Mao, Discrete plasticity in sub-10-nm-sized gold crystals, Nature Commun. 1 (2010).
[14] N.-Y. Park, H.-S. Nam, P.-R. Cha, S.-C. Lee, Size-dependent transition of the deformation behavior of Au nanowires, Nano Res. 8 (3) (2015) 941–947.
[15] J. Wang, F. Sansoz, J. Huang, Y. Liu, S. Sun, Z. Zhang, S.X. Mao, Near-ideal theoretical strength in gold nanowires containing angstrom scale twins, Nature Commun. 4 (2013) 1742.
[16] K. Cao, Y. Han, H. Zhang, L. Gao, H. Yang, J. Chen, Y. Li, Y. Lu, Size-dependent fracture behavior of silver nanowires, Nanotechnology 29 (29) (2018) 295703.
[17] M. Legros, D. Gianola, C. Motz, Quantitative in situ mechanical testing in electron microscopes, MRS Bull. 35 (5) (2010) 354–360.
[18] Q. Yu, M. Legros, A. Minor, In situ TEM nanomechanics, Mrs Bull. 40 (1) (2015) 62–70.
[19] R. Ramachandramoorthy, R. Bernal, H.D. Espinosa, Pushing the envelope of in situ transmission electron microscopy, ACS Nano 9 (5) (2015) 4675–4685.
[20] R. Schwaiger, O. Kraft, High cycle fatigue of thin silver films investigated by dynamic microbeam deflection, Scr. Mater. 41 (8) (1999) 823–829.
[21] X. Zhang, Y. He, M.L. Sushko, J. Liu, L. Luo, J.J. De Yoreo, S.X. Mao, C. Wang, K.M. Rosso, Direction-specific van der waals attraction between rutile tio2 nanocrystals, Science 356 (6336) (2017) 434–437.
[22] J. Wang, F. Sansoz, C. Deng, G. Xu, G. Han, S.X. Mao, Strong Hall-Petch type behavior in the elastic strain limit of Nanotwinned Gold Nanowires, Nano Lett. 15 (6) (2015) 3865–3870.
[23] Y. Zhu, Q. Qin, F. Xu, F. Fan, Y. Ding, T. Zhang, B.J. Wiley, Z.L. Wang, Size effects on elasticity, yielding, and fracture of silver nanowires: In situ experiments, Phys. Rev. B 85 (4) (2012) 045443.
[24] Y. Lu, J. Lou, Quantitative in-situ nanomechanical characterization of metallic nanowires, Jom 63 (9) (2011) 35.

[25] G. Cheng, C. Miao, Q. Qin, J. Li, F. Xu, H. Haftbaradaran, E.C. Dickey, H. Gao, Y. Zhu, Large anelasticity and associated energy dissipation in single-crystalline nanowires, Nature Nanotechnol. 10 (8) (2015) 687–691.
[26] G. Richter, K. Hillerich, D.S. Gianola, R. Monig, O. Kraft, C.A. Volkert, Ultrahigh strength single crystalline nanowhiskers grown by physical vapor deposition, Nano Lett. 9 (8) (2009) 3048–3052.
[27] L.H. Wang, T.J. Xin, D.L. Kong, X.Y. Shu, Y.H. Chen, H. Zhou, J. Teng, Z. Zhang, J. Zou, X.D. Han, In situ observation of stress induced grain boundary migration in nanocrystalline gold, Scr. Mater. 134 (2017) 95–99.
[28] M. Legros, D.S. Gianola, K.J. Hemker, In situ TEM observations of fast grain-boundary motion in stressed nanocrystalline aluminum films, Acta Mater. 56 (14) (2008) 3380–3393.
[29] L. Wang, J. Teng, P. Liu, A. Hirata, E. Ma, Z. Zhang, M. Chen, X. Han, Grain rotation mediated by grain boundary dislocations in nanocrystalline platinum, Nature Commun. 5 (2014) 4402.
[30] O. Kraft, M. Hommel, E. Arzt, X-ray diffraction as a tool to study the mechanical behaviour of thin films, Mater. Sci. Eng. A 288 (2) (2000) 209–216.
[31] Z.W. Shan, R.K. Mishra, S.A. Syed Asif, O.L. Warren, A.M. Minor, Mechanical annealing and source-limited deformation in submicrometre-diameter Ni crystals, Nature Mater. 7 (2) (2008) 115–119.
[32] Z.J. Wang, Q.J. Li, Y.N. Cui, Z.L. Liu, E. Ma, J. Li, J. Sun, Z. Zhuang, M. Dao, Z.W. Shan, S. Suresh, Cyclic deformation leads to defect healing and strengthening of small-volume metal crystals, Proc. Natl. Acad. Sci. USA 112 (44) (2015) 13502–13507.
[33] D. Kiener, C. Motz, M. Rester, M. Jenko, G. Dehm, FIB damage of Cu and possible consequences for miniaturized mechanical tests, Mater. Sci. Eng. A 459 (1–2) (2007) 262–272.
[34] S. Yin, G. Cheng, G. Richter, H. Gao, Y. Zhu, Transition of deformation mechanisms in single-crystalline metallic nanowires, ACS Nano 13 (8) (2019) 9082–9090.
[35] H.D. Espinosa, R.A. Bernal, T. Filleter, In situ TEM electromechanical testing of nanowires and nanotubes, Small 8 (21) (2012) 3233–3252.
[36] L. Zhong, F. Sansoz, Y. He, C. Wang, Z. Zhang, S.X. Mao, Slip-activated surface creep with room-temperature super-elongation in metallic nanocrystals, Nature Mater. 16 (4) (2017) 439–445.
[37] J. Wang, Z. Zeng, C.R. Weinberger, Z. Zhang, T. Zhu, S.X. Mao, In situ atomic-scale observation of twinning-dominated deformation in nanoscale body-centred cubic tungsten, Nature Mater. 14 (6) (2015) 594–600.
[38] Q. Zhu, G. Cao, J. Wang, C. Deng, J. Li, Z. Zhang, S.X. Mao, In situ atomistic observation of disconnection-mediated grain boundary migration, Nature Commun. 10 (1) (2019) 156.
[39] L. Zhong, J. Wang, H. Sheng, Z. Zhang, S.X. Mao, Formation of monatomic metallic glasses through ultrafast liquid quenching, Nature 512 (7513) (2014) 177.
[40] J. Wang, Y. Wang, W. Cai, J. Li, Z. Zhang, S.X. Mao, Discrete shear band plasticity through dislocation activities in body-centered cubic tungsten nanowires, Sci. Rep. 8 (2018).
[41] Q. Qin, S. Yin, G. Cheng, X. Li, T.-H. Chang, G. Richter, Y. Zhu, H. Gao, Recoverable plasticity in penta-twinned metallic nanowires governed by dislocation nucleation and retraction, Nature Commun. 6 (1) (2015) 1–8.
[42] T. Ohmura, A. Minor, E. Stach, J. Morris, Dislocation–grain boundary interactions in martensitic steel observed through in situ nanoindentation in a transmission electron microscope, J. Mater. Res. 19 (12) (2004) 3626–3632.
[43] M. Bobji, C. Ramanujan, J. Pethica, B. Inkson, A miniaturized TEM nanoindenter for studying material deformation in situ, Meas. Sci. Technol. 17 (6) (2006) 1324.
[44] Y. Lu, J.Y. Huang, C. Wang, S. Sun, J. Lou, Cold welding of ultrathin gold nanowires, Nature Nanotechnol. 5 (3) (2010) 218.
[45] J. Wang, S.X. Mao, Atomistic perspective on in situ nanomechanics, Extreme Mech. Lett. 8 (2016) 127–139.
[46] Wang Lihua, Han Xiaodong, Liu Pan, Yue Yonghai, Zhang Ze, Ma En, Wang lihua han xiaodong liu pan yue yonghai zhang ze ma en in situ observation of dislocation behavior in nanometer grains, Phys. Rev. Lett. 105 (2010) 135501.
[47] Wang Lihua, Teng Jiao, Wu Yu, Sha Xuechao, Xiang Sisi, Mao Shengcheng, Yu Guanghua, Zhang Ze, Zou Jin, Han Xiaodong, Wang lihua teng jiao wu yu sha xuechao xiang sisi mao shengcheng yu guanghua zhang ze zou jin han xiaodong in situ atomic scale mechanisms of strain-induced twin boundary shear to high angle grain boundary in nanocrystalline pt, Ultramicroscopy 195 (2018) 69–73.
[48] S. Sun, D. Kong, D. Li, X. Liao, D. Liu, S. Mao, Z. Zhang, L. Wang, X. Han, Atomistic mechanism of stress-induced combined slip and diffusion in Sub-5 Nanometer-Sized Ag nanowires, ACS Nano 13 (8) (2019) 8708–8716.
[49] Wang Lihua, Teng Jiao, Wu Yu, Zou Jin, Yu Guanghua, Zhang Ze, Han Xiaodong, Wang lihua teng jiao wu yu zou jin yu guanghua zhang ze han xiaodong size dependence of dislocation activities and independence on theoretical elastic strain limit in pt nanocrystals revealed by atomic-resolution in situ investigation, Materials Today Nano 2 (2018) 1–6.
[50] H. Zheng, J. Wang, J.Y. Huang, J. Wang, S.X. Mao, Void-assisted plasticity in Ag nanowires with a single twin structure, Nanoscale 6 (16) (2014) 9574–9578.
[51] G. Cao, J. Wang, K. Du, X. Wang, J. Li, Z. Zhang, S.X. Mao, Superplasticity in Gold Nanowires through the operation of multiple slip systems, Adv. Funct. Mater. 28 (51) (2018) 1805258.
[52] J.Y. Zhang, X. Zhang, G. Liu, R.H. Wang, G.J. Zhang, J. Sun, Length scale dependent yield strength and fatigue behavior of nanocrystalline Cu thin films, Mater. Sci. Eng. A 528 (25–26) (2011) 7774–7780.
[53] P.M. Anderson, J.P. Hirth, J. Lothe, Theory of Dislocations, third ed., Cambridge University Press, New York, USA, 2017.
[54] V. Yamakov, D. Wolf, S. Phillpot, A. Mukherjee, H. Gleiter, Deformation-mechanism map for nanocrystalline metals by molecular-dynamics simulation, Nature Mater. 3 (1) (2004) 43.
[55] J. Schiøtz, K.W. Jacobsen, A maximum in the strength of nanocrystalline copper, Science 301 (5638) (2003) 1357–1359.
[56] X. Li, Y. Wei, L. Lu, K. Lu, H. Gao, Dislocation nucleation governed softening and maximum strength in nano-twinned metals, Nature 464 (7290) (2010) 877.
[57] L. Lu, X. Chen, X. Huang, K. Lu, Revealing the maximum strength in nanotwinned copper, Science 323 (5914) (2009) 607–610.
[58] L. Lu, M. Dao, T. Zhu, J. Li, Size dependence of rate-controlling deformation mechanisms in nanotwinned copper, Scr. Mater. 60 (12) (2009) 1062–1066.
[59] L. Lu, R. Schwaiger, Z. Shan, M. Dao, K. Lu, S. Suresh, Nano-sized twins induce high rate sensitivity of flow stress in pure copper, Acta Mater. 53 (7) (2005) 2169–2179.
[60] L. Lu, T. Zhu, Y. Shen, M. Dao, K. Lu, S. Suresh, Stress relaxation and the structure size-dependence of plastic deformation in nanotwinned copper, Acta Mater. 57 (17) (2009) 5165–5173.
[61] C. Chisholm, H. Bei, M. Lowry, J. Oh, S.S. Asif, O. Warren, Z. Shan, E.P. George, A.M. Minor, Dislocation starvation and exhaustion hardening in Mo alloy nanofibers, Acta Mater. 60 (5) (2012) 2258–2264.
[62] D. Kiener, A. Minor, Source truncation and exhaustion: insights from quantitative in situ TEM tensile testing, Nano Lett. 11 (9) (2011) 3816–3820.
[63] S.H. Oh, M. Legros, D. Kiener, G. Dehm, In situ observation of dislocation nucleation and escape in a submicrometre aluminium single crystal, Nature Mater. 8 (2) (2009) 95.
[64] F. Mompiou, M. Legros, A. Sedlmayr, D.S. Gianola, D. Caillard, O. Kraft, Source-based strengthening of sub-micrometer Al fibers, Acta Mater. 60 (3) (2012) 977–983.
[65] T.A. Parthasarathy, S.I. Rao, D.M. Dimiduk, M.D. Uchic, D.R. Trinkle, Contribution to size effect of yield strength from the stochastics of dislocation source lengths in finite samples, Scr. Mater. 56 (4) (2007) 313–316.
[66] J.R. Greer, C.R. Weinberger, W. Cai, Comparing the strength of fcc and bcc sub-micrometer pillars: Compression experiments and dislocation dynamics simulations, Mater. Sci. Eng. A 493 (1–2) (2008) 21–25.
[67] J.Y. Kim, D.C. Jong, J.R. Greer, Tensile and compressive behavior of tungsten, molybdenum, tantalum and niobium at the nanoscale, Acta Mater. 58 (7) (2010) 2355–2363.
[68] C.R. Weinberger, W. Cai, Surface-controlled dislocation multiplication in metal micropillars, Proc. Natl. Acad. Sci. 105 (38) (2008) 14304–14307.
[69] L. Huang, Q.J. Li, Z.W. Shan, J. Li, J. Sun, E. Ma, A new regime for mechanical annealing and strong sample-size strengthening in body centred cubic molybdenum, Nature Commun. 2 (2011) 547.
[70] S. Brinckmann, J.-Y. Kim, J.R. Greer, Fundamental differences in mechanical behavior between two types of crystals at the nanoscale, Phys. Rev. Lett. 100 (15) (2008) 155502.
[71] A.S. Schneider, D. Kaufmann, B.G. Clark, C.P. Frick, P.A. Gruber, R. Monig, O. Kraft, E. Arzt, Correlation between critical temperature and strength of small-scale bcc pillars, Phys. Rev. Lett. 103 (10) (2009) 105501.
[72] M.D. Uchic, D.M. Dimiduk, J.N. Florando, W.D. Nix, Sample dimensions influence strength and crystal plasticity, Science 305 (5686) (2004) 986–989.
[73] J.R. Greer, W.D. Nix, Nanoscale gold pillars strengthened through dislocation starvation, Phys. Rev. B 73 (24) (2006) 245410.
[74] T. Filleter, S. Ryu, K. Kang, J. Yin, R.A. Bernal, K. Sohn, S. Li, J. Huang, W. Cai, H.D. Espinosa, Nucleation-controlled distributed plasticity in penta-twinned silver nanowires, Small 8 (19) (2012) 2986–2993.
[75] G. Cheng, S. Yin, T.-H. Chang, G. Richter, H. Gao, Y. Zhu, Anomalous tensile detwinning in twinned nanowires, Phys. Rev. Lett. 119 (25) (2017) 256101.

[76] R. Ramachandramoorthy, W. Gao, R. Bernal, H. Espinosa, High strain rate tensile testing of silver nanowires: rate-dependent brittle-to-ductile transition, Nano Lett. 16 (1) (2015) 255–263.
[77] S.H. Oh, M. Legros, D. Kiener, P. Gruber, G. Dehm, In situ TEM straining of single crystal au films on polyimide: Change of deformation mechanisms at the nanoscale, Acta Mater. 55 (16) (2007) 5558–5571.
[78] B. Hwang, M. Kang, S. Lee, C.R. Weinberger, P. Loya, J. Lou, S.H. Oh, B. Kim, S.M. Han, Effect of surface energy on size-dependent deformation twinning of defect-free Au nanowires, Nanoscale 7 (38) (2015) 15657–15664.
[79] Lu Yang, Song Jun, Huang Jianyu, Lou Jun, Lu yang song jun huang jianyu lou jun fracture of sub-20nm ultrathin gold nanowires, Adv. Funct. Mater. 21 (2011) 3982–3989.
[80] Q. Li, B. Xu, S. Hara, J. Li, E. Ma, Sample-size-dependent surface dislocation nucleation in nanoscale crystals, Acta Mater. 145 (2018) 19–29.
[81] J.-H. Seo, H.S. Park, Y. Yoo, T.-Y. Seong, J. Li, J.-P. Ahn, B. Kim, I.-S. Choi, Origin of size dependency in coherent-twin-propagation-mediated tensile deformation of noble metal nanowires, Nano Lett. 13 (11) (2013) 5112–5116.
[82] L.Y. Chen, M.R. He, J. Shin, G. Richter, D.S. Gianola, Measuring surface dislocation nucleation in defect-scarce nanostructures, Nature Mater. 14 (7) (2015) 707–713.
[83] L. Wang, J. Teng, D. Kong, G. Yu, J. Zou, Z. Zhang, X. Han, In situ atomistic deformation mechanisms of twin-structured nanocrystal Pt, Scr. Mater. 147 (2018) 103–107.
[84] L. Wang, K. Du, C. Yang, J. Teng, L. Fu, Y. Guo, Z. Zhang, X. Han, In situ atomic-scale observation of grain size and twin thickness effect limit in twin-structural nanocrystalline platinum, Nature Commun. 11 (1) (2020) 1–9.
[85] L. Wang, P. Guan, J. Teng, P. Liu, D. Chen, W. Xie, D. Kong, S. Zhang, T. Zhu, Z. Zhang, New twinning route in face-centered cubic nanocrystalline metals, Nature Commun. 8 (1) (2017) 2142.
[86] J.-H. Seo, Y. Yoo, N.-Y. Park, S.-W. Yoon, H. Lee, S. Han, S.-W. Lee, T.-Y. Seong, S.-C. Lee, K.-B. Lee, Superplastic deformation of defect-free au nanowires via coherent twin propagation, Nano Lett. 11 (8) (2011) 3499–3502.
[87] B. Li, B. Li, Y. Wang, M. Sui, E. Ma, Twinning mechanism via synchronized activation of partial dislocations in face-centered-cubic materials, Scr. Mater. 64 (9) (2011) 852–855.
[88] C. Marichal, H. Van Swygenhoven, S. Van Petegem, C. Borca, {110} Slip with {112} slip traces in bcc Tungsten, Sci. Rep.-Uk 3 (2013) 2547.
[89] S. Min Han, G. Feng, J. Young Jung, H. Joon Jung, J.R. Groves, W.D. Nix, Y. Cui, Critical-temperature/Peierls-stress dependent size effects in body centered cubic nanopillars, Appl. Phys. Lett. 102 (4) (2013) 041910.
[90] D. Caillard, Kinetics of dislocations in pure Fe. Part I. In situ straining experiments at room temperature, Acta Mater. 58 (9) (2010) 3493–3503.
[91] Q. Wang, J. Wang, J. Li, Z. Zhang, S.X. Mao, Consecutive crystallographic reorientations and superplasticity in body-centered cubic niobium nanowires, Sci. Adv. 4 (7) (2018).
[92] M.A. Meyers, K.K. Chawla, Mechanical Behavior of Materials, Cambridge university press, 2008.
[93] S. Lee, J. Im, Y. Yoo, E. Bitzek, D. Kiener, G. Richter, B. Kim, S.H. Oh, Reversible cyclic deformation mechanism of gold nanowires by twinning–detwinning transition evidenced from in situ TEM, Nature Commun. 5 (2014) 3033.
[94] B. Roos, B. Kapelle, G. Richter, C. Volkert, Surface dislocation nucleation controlled deformation of Au nanowires, Appl. Phys. Lett. 105 (20) (2014) 201908.
[95] S. Wei, Q. Wang, H. Wei, J. Wang, Bending-induced deformation twinning in body-centered cubic tungsten nanowires, Mater. Res. Lett. 7 (5) (2019) 210–216.
[96] Y. Yue, P. Liu, Q. Deng, E. Ma, Z. Zhang, X. Han, Quantitative evidence of crossover toward partial dislocation mediated plasticity in copper single crystalline nanowires, Nano Lett. 12 (8) (2012) 4045–4049.
[97] A. Sedlmayr, E. Bitzek, D.S. Gianola, G. Richter, R. Mönig, O. Kraft, Existence of two twinning-mediated plastic deformation modes in Au nanowhiskers, Acta Mater. 60 (9) (2012) 3985–3993.
[98] J. Wang, G. Cao, Z. Zhang, F. Sansoz, Size-dependent dislocation–twin interactions, Nanoscale 11 (26) (2019) 12672–12679.
[99] L. Wang, Y. Lu, D. Kong, L. Xiao, X. Sha, J. Sun, Z. Zhang, X. Han, Dynamic and atomic-scale understanding of the twin thickness effect on dislocation nucleation and propagation activities by in situ bending of Ni nanowires, Acta Mater. 90 (2015) 194–203.
[100] D. Jang, X. Li, H. Gao, J.R. Greer, Deformation mechanisms in nanotwinned metal nanopillars, Nature Nanotechnol. 7 (9) (2012) 594.
[101] Li Jiao, Zhang Jinyu, Liu Gang, Sun Jun, Using the room temperature creep to strengthen nanotwinned ni: the scaling behavior between the twin thickness and the grain size, Mater. Today Nano 11 (2020) 100086.
[102] J. Wang, N. Li, O. Anderoglu, X. Zhang, A. Misra, J. Huang, J. Hirth, Detwinning mechanisms for growth twins in face-centered cubic metals, Acta Mater. 58 (6) (2010) 2262–2270.
[103] Fu Xiaoqian, Wu Xiaolei, Yu Qian, Fu xiaoqian wu xiaolei yu qian dislocation plasticity reigns in a traditional twinning-induced plasticity steel by in situ observation, Mater. Today Nano 3 (2018) 48–53.
[104] Wang Lihua, Kong Deli, Zhang Yin, Xiao Lirong, Lu Yan, Chen Zhigang, Zhang Ze, Zou Jin, Zhu Ting, Han Xiaodong, Wang lihua kong deli zhang yin xiao lirong lu yan chen zhigang zhang ze zou jin zhu ting han xiaodong mechanically driven grain boundary formation in nickel nanowires, ACS Nano 11 (2017) 12500–12508.
[105] J. Diao, K. Gall, M.L. Dunn, Surface stress driven reorientation of gold nanowires, Phys. Rev. B 70 (7) (2004) 075413.
[106] J. Diao, K. Gall, M.L. Dunn, Surface-stress-induced phase transformation in metal nanowires, Nature Mater. 2 (10) (2003) 656.
[107] A. Nie, H. Wang, Deformation-mediated phase transformation in gold nano-junction, Mater. Lett. 65 (23–24) (2011) 3380–3383.
[108] L. Wang, P. Liu, P. Guan, M. Yang, J. Sun, Y. Cheng, A. Hirata, Z. Zhang, E. Ma, M. Chen, In situ atomic-scale observation of continuous and reversible lattice deformation beyond the elastic limit, Nature Commun. 4 (2013) 2413.
[109] Z. Nishiyama, X-ray investigation of the mechanism of the transformation from face centered cubic lattice to body centered cubic, Sci. Rep. Tohoku Univ. 23 (1934) 637–664.
[110] G. Kurdjumov, G. Sachs, Over the mechanisms of steel hardening, Z. Phys. 64 (1930) 325–343.
[111] Y. Lu, S. Xiang, L. Xiao, L. Wang, Q. Deng, Z. Zhang, X. Han, Dislocation bubble-like-effect and the ambient temperature super-plastic elongation of body-centred cubic single crystalline molybdenum, Sci. Rep. 6 (2016) 22937.
[112] S.J. Wang, H. Wang, K. Du, W. Zhang, M.L. Sui, S.X. Mao, Deformation-induced structural transition in body-centred cubic molybdenum, Nature Commun. 5 (2014).
[113] D. Chachamovitz, D. Mordehai, The stress-dependent activation parameters for dislocation nucleation in molybdenum nanoparticles, Sci. Rep. 8 (1) (2018) 3915.
[114] T. Zhu, J. Li, Ultra-strength materials, Prog. Mater. Sci. 55 (7) (2010) 710–757.
[115] J. Diao, K. Gall, M.L. Dunn, J.A. Zimmerman, Atomistic simulations of the yielding of gold nanowires, Acta Mater. 54 (3) (2006) 643–653.
[116] J. Diao, K. Gall, M.L. Dunn, Yield strength asymmetry in metal nanowires, Nano Lett. 4 (10) (2004) 1863–1867.
[117] A.T. Jennings, C.R. Weinberger, S.-W. Lee, Z.H. Aitken, L. Meza, J.R. Greer, Modeling dislocation nucleation strengths in pristine metallic nanowires under experimental conditions, Acta Mater. 61 (6) (2013) 2244–2259.
[118] C.R. Weinberger, A.T. Jennings, K. Kang, J.R. Greer, Atomistic simulations and continuum modeling of dislocation nucleation and strength in gold nanowires, J. Mech. Phys. Solids 60 (1) (2012) 84–103.
[119] L. Tian, J. Li, J. Sun, E. Ma, Z.W. Shan, Visualizing size-dependent deformation mechanism transition in Sn, Sci. Rep.-Uk 3 (2013) 2113.
[120] H. Göbel, P. Von Blanckenhagen, A study of surface diffusion on gold with an atomic force microscope, Surf. Sci. 331 (1995) 885–890.
[121] H. Brune, K. Bromann, H. Röder, K. Kern, J. Jacobsen, P. Stoltze, K. Jacobsen, J. No, Effect of strain on surface diffusion and nucleation, Phys. Rev. B 52 (20) (1995) R14380.
[122] J. Sun, L. He, Y.C. Lo, T. Xu, H. Bi, L. Sun, Z. Zhang, S.X. Mao, J. Li, Liquid-like pseudoelasticity of sub-10-nm crystalline silver particles, Nature Mater. 13 (11) (2014) 1007–1012.
[123] D. Kong, T. Xin, S. Sun, Y. Lu, X. Shu, H. Long, Y. Chen, J. Teng, Z. Zhang, L. Wang, Surface energy driven Liquid-Drop-Like pseudoelastic behaviors and In Situ Atomistic Mechanisms of Small-Sized face-Centered-Cubic Metals, Nano Lett. 19 (1) (2018) 292–298.
[124] B. Arab, S. Sanjabi, A. Shokuhfar, Size dependency of self-diffusion and creep behavior of nanostructured metals, Mater. Lett. 65 (4) (2011) 712–715.
[125] J.H. Schneibel, C.T. Liu, M.K. Miller, M.J. Mills, P. Sarosi, M. Heilmaier, D. Sturm, Ultrafine-grained nanocluster-strengthened alloys with unusually high creep strength, Scr. Mater. 61 (8) (2009) 793–796.
[126] L. Lu, M.L. Sui, K. Lu, Superplastic extensibility of nanocrystalline copper at room temperature, Science 287 (5457) (2000) 1463–1466.
[127] Q.J. Li, E. Ma, When 'smaller is stronger' no longer holds, Mater. Res. Lett. 6 (5) (2018) 283–292.
[128] D.R. Strachan, D.E. Smith, M.D. Fischbein, D.E. Johnston, B.S. Guiton, M. Drndić, D.A. Bonnell, A.T. Johnson, Clean electromigrated nanogaps imaged by transmission electron microscopy, Nano Lett. 6 (3) (2006) 441–444.
[129] B. Wang, Y. Han, S. Xu, L. Qiu, F. Ding, J. Lou, Y. Lu, Mechanically assisted Self-Healing of ultrathin gold nanowires, Small 14 (20) (2018) 1704085.
[130] V. Rodrigues, T. Fuhrer, D. Ugarte, Signature of atomic structure in the quantum conductance of gold nanowires, Phys. Rev. Lett. 85 (19) (2000) 4124.
[131] Y. Yue, P. Liu, Z. Zhang, X. Han, E. Ma, Approaching the theoretical elastic strain limit in copper nanowires, Nano Lett. 11 (8) (2011) 3151–3155.

[132] J. Li, S. Sarkar, W.T. Cox, T.J. Lenosky, E. Bitzek, Y. Wang, Diffusive molecular dynamics and its application to nanoindentation and sintering, Phys. Rev. B 84 (5) (2011) 054103.
[133] W. Liang, M. Zhou, Atomistic simulations reveal shape memory of fcc metal nanowires, Phys. Rev. B 73 (11) (2006) 115409.
[134] W. Liang, M. Zhou, F. Ke, Shape memory effect in Cu nanowires, Nano Lett. 5 (10) (2005) 2039–2043.
[135] A. Cao, Shape memory effects and pseudoelasticity in bcc metallic nanowires, J. Appl. Phys. 108 (11) (2010) 113531.
[136] W. Liang, M. Zhou, Discovery, characterization and modelling of novel shape memory behaviour of fcc metal nanowires, Phil. Mag. 87 (14–15) (2007) 2191–2220.
[137] H.S. Park, K. Gall, J.A. Zimmerman, Shape memory and pseudoelasticity in metal nanowires, Phys. Rev. Lett. 95 (25) (2005) 255504.
[138] R. Rezaei, C. Deng, Pseudoelasticity and shape memory effects in cylindrical FCC metal nanowires, Acta Mater. 132 (2017) 49–56.
[139] J. Zhu, D. Shi, Reorientation mechanisms and pseudoelasticity in iron nanowires, J. Phys. D: Appl. Phys. 44 (5) (2011) 055404.
[140] W. Liang, D.J. Srolovitz, M. Zhou, A micromechanical continuum model for the tensile behavior of shape memory metal nanowires, J. Mech. Phys. Solids 55 (8) (2007) 1729–1761.
[141] H. Zheng, J. Wang, J.Y. Huang, A. Cao, S.X. Mao, In situ visualization of Birth and Annihilation of grain boundaries in an Au Nanocrystal, Phys. Rev. Lett. 109 (22) (2012).
[142] B.Q. Li, M.L. Sui, B. Li, E. Ma, S.X. Mao, Reversible twinning in pure aluminum, Phys. Rev. Lett. 102 (20) (2009) 205504.
[143] B.Q. Li, M.L. Sui, S.X. Mao, Pseudoelastic stacking fault and deformation twinning in nanocrystalline Ni, Appl. Phys. Lett. 97 (24) (2010).
[144] B. Jiang, A. Tu, H. Wang, H. Duan, S. He, H. Ye, K. Du, Direct observation of deformation twinning under stress gradient in body-centered cubic metals, Acta Mater. 155 (2018) 56–68.
[145] Y. Zhang, P.C. Millett, M. Tonks, S. Biner, Deformation twins in nanocrystalline body-centered cubic Mo as predicted by molecular dynamics simulations, Acta Mater. 60 (18) (2012) 6421–6428.
[146] X. Wang, J. Wang, Y. He, C. Wang, L. Zhong, S.X. Mao, Unstable twin in body-centered cubic tungsten nanocrystals, Nature Commun. 11 (1) (2020) 1–7.
[147] A. Misra, J.P. Hirth, R.G. Hoagland, Length-scale-dependent deformation mechanisms in incoherent metallic multilayered composites, Acta Mater. 53 (18) (2005) 4817–4824.
[148] Y.P. Li, G.P. Zhang, On plasticity and fracture of nano structured Cu/X (X = Au, Cr) multilayers: The effects of length scale and interface/boundary, Acta Mater. 58 (11) (2010) 3877–3887.
[149] Y.P. Li, G.P. Zhang, W. Wang, J. Tan, S.J. Zhu, On interface strengthening ability in metallic multilayers, Scr. Mater. 57 (2) (2007) 117–120.
[150] J.W. Yan, G.P. Zhang, X.F. Zhu, H.S. Liu, C. Yan, Microstructures and strengthening mechanisms of Cu/Ni/W nanolayered composites, Phil. Mag. 93 (5) (2013) 434–448.
[151] N. Li, J. Wang, A. Misra, J.Y. Huang, Direct observations of confined layer slip in Cu/Nb multilayers, Microsc. Microanal. 18 (5) (2012) 1155–1162.
[152] X.M. Luo, X. Li, G.P. Zhang, Forming incoherent twin boundaries: a new way for nanograin growth under cyclic loading, Mater. Res. Lett. 5 (2) (2017) 95–101.
[153] J.W. Cahn, Y. Mishin, A. Suzuki, Coupling grain boundary motion to shear deformation, Acta Mater. 54 (19) (2006) 4953–4975.
[154] O. Renk, A. Hohenwarter, S. Wurster, R. Pippan, Direct evidence for grain boundary motion as the dominant restoration mechanism in the steady-state regime of extremely cold-rolled copper, Acta Mater. 77 (100) (2014) 401–410.
[155] D. Caillard, F. Mompiou, M. Legros, Grain-boundary shear-migration coupling. II. Geometrical model for general boundaries, Acta Mater. 57 (8) (2009) 2390–2402.
[156] Z. Zhang, H. Sheng, Z. Wang, B. Gludovatz, Z. Zhang, E.P. George, Q. Yu, S.X. Mao, R.O. Ritchie, Dislocation mechanisms and 3D twin architectures generate exceptional strength-ductility-toughness combination in CrCoNi medium-entropy alloy, Nature Commun. 8 (2017).
[157] Z. Zhang, M.M. Mao, J. Wang, B. Gludovatz, Z. Zhang, S.X. Mao, E.P. George, Q. Yu, R.O. Ritchie, Nanoscale origins of the damage tolerance of the high-entropy alloy CrMnFeCoNi, Nature Commun. 6 (2015).
[158] M. Naeem, H. He, F. Zhang, H. Huang, S. Harjo, T. Kawasaki, B. Wang, S. Lan, Z. Wu, F. Wang, Cooperative deformation in high-entropy alloys at ultralow temperatures, Sci. Adv. 6 (13) (2020) eaax4002.
[159] Q. Ding, Y. Zhang, X. Chen, X. Fu, D. Chen, S. Chen, L. Gu, F. Wei, H. Bei, Y. Gao, Tuning element distribution, structure and properties by composition in high-entropy alloys, Nature 574 (7777) (2019) 223–227.
[160] X. Du, W. Li, H. Chang, T. Yang, G. Duan, B. Wu, J. Huang, F. Chen, C. Liu, W. Chuang, Dual heterogeneous structures lead to ultrahigh strength and uniform ductility in a Co-Cr-Ni medium-entropy alloy, Nature Commun. 11 (1) (2020) 1–7.
[161] F.G. Sen, A.T. Alpas, A.C. Van Duin, Y. Qi, Oxidation-assisted ductility of aluminium nanowires, Nature Commun. 5 (1) (2014) 1–9.
[162] J. Shin, L.Y. Chen, U.T. Sanli, G. Richter, S. Labat, M.-I. Richard, T. Cornelius, O. Thomas, D.S. Gianola, Controlling dislocation nucleation-mediated plasticity in nanostructures via surface modification, Acta Mater. 166 (2019) 572–586.